

COMPUTER SIMULATION OF CIRCULAR DICHROISM AND
OPTICAL ROTATORY DISPERSION.

by

M. W. Evans¹,
Institute of Physical Chemistry,
University of Zürich,
Winterthurerstraße 190,
CH 8057 Zürich,
Switzerland.

¹ Permanent address: 433 Theory Center, Cornell University, Ithaca, NY
14853, U.S.A.

(Received 5 June 1991)

ABSTRACT

Field applied molecular dynamics (FMD) computer simulation is used to reveal the molecular dynamical nature of circular dichroism (CD) and optical rotatory dispersion (ORD). The set of pseudo-scalar T positive and P negative difference time correlation functions (DCF's) is introduced as a means of quantifying the different torques set up by the interaction of left and right circularly polarised electromagnetic radiation with an ensemble of chiral molecules. The torque difference is proportional to the anisotropy of the Rosenfeld tensor in the molecule fixed frame and is accompanied by frequency doubling. FMD simulation is carried out for laser and broad band radiation for a rigid and chiral molecular structure, that of bromochlorofluoromethane, i.e. attention is restricted to translational, rotational and re-orientational dynamics without considering molecular vibration.

INTRODUCTION

It is well known that left and right circularly polarised electromagnetic plane waves interact differently with a chiral ("optically active") molecular structure. This gives rise to circular dichroism (CD) and optical rotatory dispersion (ORD) across the complete electromagnetic spectrum. Contemporary semi-classical descriptions {1-3} express CD and

ORD in terms of the g and f components, respectively, of the imaginary part of the Rosenfeld molecular property tensor:

$$\langle A_{LZ} - A_{RZ} \rangle = 4\omega\mu_0 N \langle \alpha_{2\alpha\beta}^H(g) \rangle \quad (1)$$

$$\langle \theta \rangle = -l\mu_0 N \omega \langle \alpha_{2\alpha\beta}^H(f) \rangle \quad (2)$$

Here, f and g are the dispersive and absorptive bandshape functions respectively. $\langle A_{LZ} - A_{RZ} \rangle$ is the difference in the power absorption coefficient (neper per centimetre) measured respectively with left and right circularly polarised radiation propagating in the Z axis of the laboratory frame (X, Y, Z); and $\langle \theta \rangle$ the corresponding difference in radians in the angle of rotation of the plane of linear polarisation. (A linearly polarised electromagnetic plane wave is 50% left and 50% right circularly polarised.) N is the number of molecules per cubic metre; ω is the angular frequency in radians per second of the wave; μ_0 is the vacuum permeability ($4\pi \times 10^{-7} \text{Js}^{-2}\text{C}^{-2}$) and l the sample length in metres. The angular brackets $\langle \quad \rangle$ denote ensemble averaging [4]. The imaginary part, $\alpha_{2\alpha\beta}^H$, of the Rosenfeld tensor is responsible both for CD and ORD, and is well defined [1-3] in semi-classical theory and density matrix formalism as being proportional to a product of matrix elements of the magnetic and electric molecular electronic dipole moments. It is positive to motion reversal (T) and negative to parity inversion (P). Individual cartesian components both of $\alpha_{2\alpha\beta}^H(g)$ and $\alpha_{2\alpha\beta}^H(f)$ have, in consequence, the symmetry of a pseudo-scalar, which changes sign between enantiomorphs of a chiral molecule. Thus, CD and ORD also change sign when an enantiomeric ensemble is replaced by its mirror image, and vanish in the racemic mixture.

This paper investigates the classical molecular dynamical processes at the root of CD and ORD in ensembles of rigid chiral molecules exemplified by the C_1 symmetry bromochlorofluoromethanes. It uses field applied molecular dynamics computer simulation (FMD) [5-10] to define a novel set of pseudo-scalar, T positive, P negative, difference time correlation functions (DCF's) of an ensemble of chiral molecules in the presence of a plane polarised electromagnetic wave. The different interactions with the chiral ensemble of the left and right components of this wave are expressed as different torques. The latter are worked out in section 1 and coded into the forces loop of an FMD simulation algorithm, described in section 3. The torque difference set up between left and right

circularly polarised plane waves and the chiral molecular structure is shown in section 1 to depend on the anisotropy of diagonal, or principal, elements of α_{ij}'' in a frame (1,2,3) fixed in the molecule. This frame is conveniently approximated by that of the principal molecular moments of inertia. It follows that the torque difference is zero: 1) if there is no anisotropy in the Rosenfeld tensor; 2) if the molecule is achiral, so that all elements of the Rosenfeld tensor vanish independently. When the torque difference is zero, there is no CD or ORD, and no DCF's.

Section 2 discusses some of the molecular dynamical implications of the torque difference ΔT in terms of the set of DCF's. Each non-vanishing member of this set has components which are pseudo-scalars, and each emerges automatically from the FMD simulation as a consequence of ΔT . A DCF is always present as some underlying component of a CD or ORD spectrum, and exists in the laboratory frame (X, Y, Z) as a quantity generated by the interaction of plane polarised electromagnetic radiation with a chiral ensemble. The specific DCF responsible directly for CD is shown in section 2 to be a rotational velocity DCF, the Fourier transform [11] of the left hand side of eqn. [1]. Section 4 illustrates DCF's from an FMD simulation of the S and R enantiomers of bromochlorofluoromethane, modelled by a rigid site-site potential taken from the literature [12].

1. THE TORQUE DIFFERENCE, ΔT .

To work out the torque difference ΔT in a form suitable for FMD simulation we consider circular dichroism through a specific mechanism described through the induction

$$m_{\alpha}^{(R)} = \alpha_{2\alpha\beta}''(g) \text{Real} (E_{\beta}^{(R)}) \quad (3)$$

$$m_{\alpha}^{(L)} = \alpha_{2\alpha\beta}''(g) \text{Real} (E_{\beta}^{(L)}) \quad (4)$$

of a magnetic dipole moment m_0 in a given enantiomer. Here, the R and L superscripts denote right and left circularly polarised respectively. The magnetic dipole moment is produced by the product of the real quantity $\alpha_{2\alpha\beta}''(g)$ with the real parts of the electric field strengths (volts per metre)

$$\text{Real} (E^{(R)}) = E_0(i \cos \phi_R - j \sin \phi_R) \quad (5)$$

$$\text{Real} (E^{(L)}) = E_0(i \cos \phi_L + j \sin \phi_L) \quad (6)$$

respectively. The corresponding magnetic flux densities (in Tesla) are

$$\text{Real}(B^{(R)}) = B_0(i \sin \phi_R + j \cos \phi_R) \quad (7)$$

$$\text{Real}(B^{(L)}) = B_0(-i \sin \phi_L + j \cos \phi_L) \quad (8)$$

The right and left torques are consequently defined in frame (X, Y, Z) as

$$T^{(R)} = -m^{(R)} \times \text{Real}(B^{(R)}) \quad (9)$$

$$T^{(L)} = -m^{(L)} \times \text{Real}(B^{(L)}) \quad (10)$$

We have considered a plane wave propagating in the Z axis of the laboratory frame (X, Y, Z). The torque difference is, accordingly

$$\Delta T = T^{(L)} - T^{(R)} \quad (11)$$

Here i and j are unit vectors in axes X and Y respectively, i is the root of minus one, E_0 and B_0 are scalar amplitudes, and the electromagnetic phases are

$$\phi_R = \omega t - \kappa_R \cdot r \quad (12)$$

where κ_L and κ_R are respectively the left and right propagation vectors. The phases are approximated in the FMD simulation of this paper with

$$\phi_L = \omega t - \kappa_L \cdot r \quad (13)$$

$$\phi_L \approx \phi_R = \omega t \quad (14)$$

We transform this into the frame (1, 2, 3) of the principal molecular moments of inertia, a frame which is assumed to be the same as that of the principal components of α_{ij}'' . In frame (1, 2, 3) therefore

$$\begin{bmatrix} m_1 \\ m_2 \\ m_3 \end{bmatrix} = \begin{bmatrix} \alpha_{2,11}''(g) & 0 & 0 \\ 0 & \alpha_{2,22}''(g) & 0 \\ 0 & 0 & \alpha_{2,33}''(g) \end{bmatrix} \begin{bmatrix} E_1 \\ E_2 \\ E_3 \end{bmatrix} \quad (15)$$

where the electric and magnetic field components have been transformed {13-16} using

$$\begin{aligned} E_1 &= e_{1X}E_X + e_{1Y}E_Y \\ E_2 &= e_{2X}E_X + e_{2Y}E_Y \\ E_3 &= e_{3X}E_X + e_{3Y}E_Y \end{aligned} \quad (16)$$

Here e_1 , e_2 and e_3 are unit vectors in axes 1, 2, and 3 respectively. The torque components in frame (1, 2, 3) are therefore

$$\begin{aligned} T_{1L} &= \alpha''_{2,22}(g)E_{L2}B_{L3} - \alpha''_{2,33}(g)E_{L3}B_{L2} \\ T_{2L} &= \alpha''_{2,33}(g)E_{L3}B_{L1} - \alpha''_{2,11}(g)E_{L1}B_{L3} \\ T_{3L} &= \alpha''_{2,11}(g)E_{L1}B_{L2} - \alpha''_{2,22}(g)E_{L2}B_{L1} \end{aligned} \quad (17)$$

and

$$\begin{aligned} T_{1R} &= \alpha''_{2,22}(g)E_{R2}B_{R3} - \alpha''_{2,33}(g)E_{R3}B_{R2} \\ T_{2R} &= \alpha''_{2,33}(g)E_{R3}B_{R1} - \alpha''_{2,11}(g)E_{R1}B_{R3} \\ T_{3R} &= \alpha''_{2,11}(g)E_{R1}B_{R2} - \alpha''_{2,22}(g)E_{R2}B_{R1} \end{aligned} \quad (18)$$

Some algebra gives the torque difference components

$$\begin{aligned} T_{1L} - T_{1R} &= (\alpha''_{2,22}(g) - \alpha''_{2,33}(g))(e_{2Y}e_{3Y} - e_{2X}e_{3X})\sin(2\omega t)E_0B_0 \\ T_{2L} - T_{2R} &= (\alpha''_{2,33}(g) - \alpha''_{2,11}(g))(e_{3Y}e_{1Y} - e_{3X}e_{1X})\sin(2\omega t)E_0B_0 \\ T_{3L} - T_{3R} &= (\alpha''_{2,11}(g) - \alpha''_{2,22}(g))(e_{1Y}e_{2Y} - e_{1X}e_{2X})\sin(2\omega t)E_0B_0 \end{aligned} \quad (19)$$

These are finally back transformed into frame (X, Y, Z) using the transformation matrix

$$\begin{bmatrix} T_X \\ T_Y \\ T_Z \end{bmatrix} = \begin{bmatrix} e_{1X} & e_{2X} & e_{3X} \\ e_{1Y} & e_{2Y} & e_{3Y} \\ e_{1Z} & e_{2Z} & e_{3Z} \end{bmatrix} \begin{bmatrix} T_1 \\ T_2 \\ T_3 \end{bmatrix} \quad (20)$$

Note that the torque difference components depend on the anisotropy of the principal Rosenfeld tensor components, and on the frequency factor $\sin(2\omega t)$. The torque difference therefore acts at twice the angular frequency of the incoming wave. It is also useful to note that integration of the torque over configuration is the work done, which is minus the potential energy. The potential energy difference between right and left components is therefore

$$\Delta(\Delta H) = -m^{(L)} \cdot B^{(L)} + m^{(R)} \cdot B^{(R)} \quad (21)$$

For optical rotatory dispersion, replace g everywhere by f . From eqn [19] we deduce immediately that the individual torque difference components in frame (1, 2, 3) and also (X, Y, Z) are pseudo-scalar quantities, positive to T and negative to P. When incorporated in the forces loop of an FMD algorithm (section 3) they generate pseudo-scalar DCF's described in detail in section 4.

2. THE SET OF NON-VANISHING DIFFERENCE CORRELATION FUNCTIONS

In general the members of this set are defined by

$$\Delta C_{AB}(t) = \frac{[\langle A_\alpha(t)B_\beta(0) \rangle]}{[\langle A_\alpha^2 \rangle^{1/2} \langle B_\beta^2 \rangle^{1/2}]_{(L)}} - \frac{[\langle A_\alpha(t)B_\beta(0) \rangle]}{[\langle A_\alpha^2 \rangle^{1/2} \langle B_\beta^2 \rangle^{1/2}]_{(R)}} \quad (22)$$

The sub-set of difference auto-correlation functions (DACF's) is defined by the special case $A = B$ and $\alpha = \beta$. Otherwise the DCF is a cross correlation function. Both auto and cross DCF components are pseudo scalars. (Conventional ACF and CCF components are scalars [17].) In general there are many non-vanishing components of this set, all generated by the torque difference components [19]. The work reported in this paper appears to be the first to define the set of DCF's, the fundamental molecular dynamical signature of CD and ORD. All members of the set vanish in an achiral ensemble, or in a racemic mixture, and also vanish when there is no applied electromagnetic field. Clearly, CD and ORD are unobservable without the use of probe radiation and without field - molecule interactions represented by [11]. In other words there are no DCF's at field free equilibrium, and they are supported only in what we call the "field-applied" or "field-on" steady state, which is the statistically stationary state of the ensemble in the presence of electromagnetic probe radiation. This can be at one frequency, ω , (laser radiation) or can be made up of a large number of different frequencies - "broad band" radiation.

Note that DCF's can be defined either in frame (X, Y, Z), or in frame (1, 2, 3). In frame (1, 2, 3), however, there exist pseudo-scalar correlation functions [18-21] in the absence of an electromagnetic field, which switch sign between enantiomorphs [18]. These are not DCF's however, because they do not need to be generated by a torque

difference. For example, the pseudo-scalar components of the CCF between molecular linear centre of mass velocity (\mathbf{v}) and the same molecule's angular velocity, $\boldsymbol{\omega}$, exist only in frame (1, 2, 3) at field free equilibrium, and in this state change sign between enantiomorphs. The DCF

$$\Delta C_{vw}(t) = \left[\frac{\langle v_{\alpha}(t)\omega_{\beta}(0) \rangle}{\langle v_{\alpha}^2 \rangle^{1/2} \langle \omega_{\beta}^2 \rangle^{1/2}} \right]_{(L)} - \left[\frac{\langle v_{\alpha}(t)\omega_{\beta}(0) \rangle}{\langle v_{\alpha}^2 \rangle^{1/2} \langle \omega_{\beta}^2 \rangle^{1/2}} \right]_{(R)} \quad (23)$$

may, however, be induced both in frame (X, Y, Z) and (1, 2, 3) by the torque difference [19], which will change the time evolution of the original field free CCF's of frame (1, 2, 3).

The DCF directly responsible for CD is that of the rotational velocity, the time derivative [22] of the permanent molecular electric dipole moment. A conventional rotational velocity correlation function is the Fourier transform of the power absorption coefficient [22], and clearly, CD is from eqn [1] a difference in power absorption coefficients measured for the same chiral ensemble with right and left circularly polarised radiation. In section 4 it is shown that the rotational velocity DCF is one out of a large number of related DCF's, computed from the same FMD trajectories.

3. FMD SIMULATION.

The FMD method [23 - 26] was applied with ensembles of (S) and (R) bromochlorofluoromethane molecules in the liquid state at 293 K. The site-site interaction potential was used as in the literature [18]

$$\frac{\epsilon}{k}(C-C) = 35.8K; \quad \sigma(C-C) = 3.4\text{\AA};$$

$$\frac{\epsilon}{k}(H-H) = 10.0K; \quad \sigma(H-H) = 2.8\text{\AA};$$

$$\frac{\epsilon}{k}(F-F) = 54.9K; \quad \sigma(F-F) = 2.7\text{\AA};$$

$$\frac{\epsilon}{k}(Br-Br) = 218.0K; \quad \sigma(Br-Br) = 3.9\text{\AA};$$

$$\frac{\epsilon}{k}(Cl-Cl) = 158.0K; \quad \sigma(Cl-Cl) = 3.6\text{\AA};$$

$$q(C) = 0.335|e|; \quad q(F) = -0.22|e|; \quad q(H) = 0.225|e|;$$

$$q(Br) = -0.16|e|; \quad q(Cl) = -0.18|e|;$$

with Lorentz-Berthelot combining rules [18]. The torque [19] was coded into the forces loop of the algorithm TETRA, whose complete code has been given elsewhere [27] and trajectories for 108 molecules generated with a time step of 5.0 fs. Second order transient ensemble averages of the type

$$\begin{aligned} &\langle e_{1x}^2 \rangle; \langle e_{2x}^2 \rangle; \langle e_{3x}^2 \rangle \\ &\langle e_{1y}^2 \rangle; \langle e_{2y}^2 \rangle; \langle e_{3y}^2 \rangle \\ &\langle e_{1z}^2 \rangle; \langle e_{2z}^2 \rangle; \langle e_{3z}^2 \rangle \end{aligned}$$

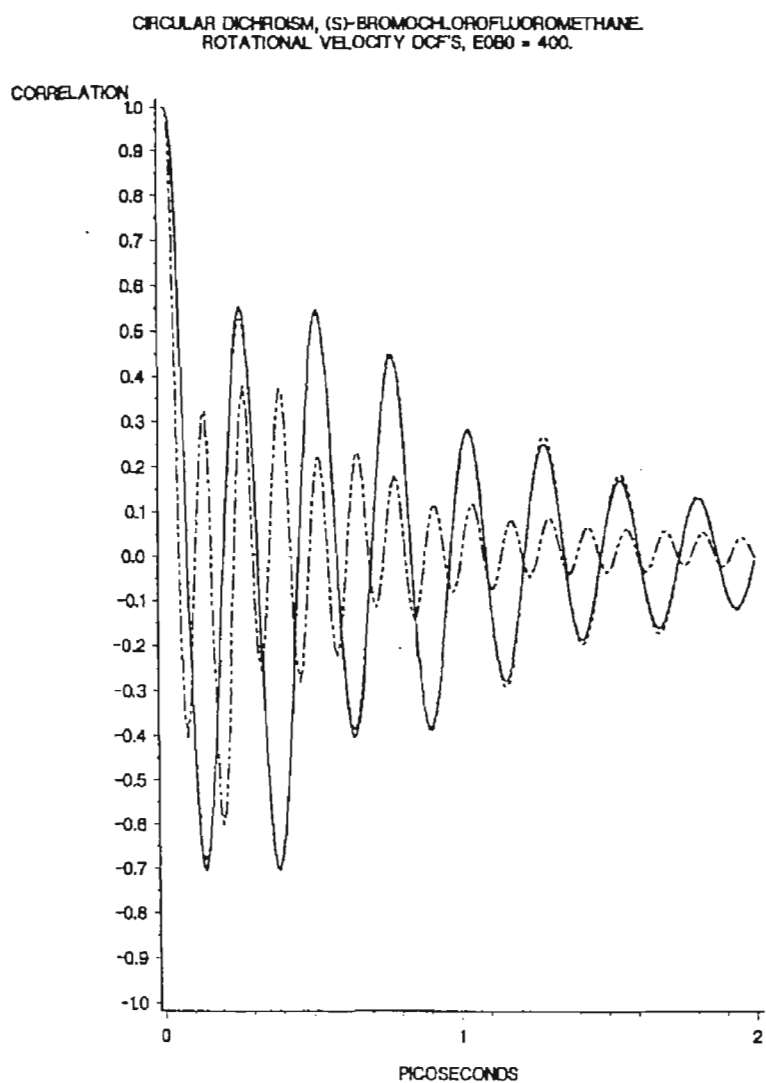


Figure 1

Rotational Velocity DCF's, _____ X component: ----- Y component;
_ .. _ .. Z component.

were recorded over 2,000 time steps, until a plateau level was reached. The latter indicates that the ensemble has reached a field-on steady state, which is statistically stationary. In this condition, DCF's were constructed by running time averaging over a span of 6,000 time steps for both enantiomers, and recorded to 400 time steps. This procedure gave "good statistics" and clearly isolated each DCF above the statistical noise.

In coding the torque [19] the following numbers were used in the absence of ab initio or experimental data on the anisotropy of the

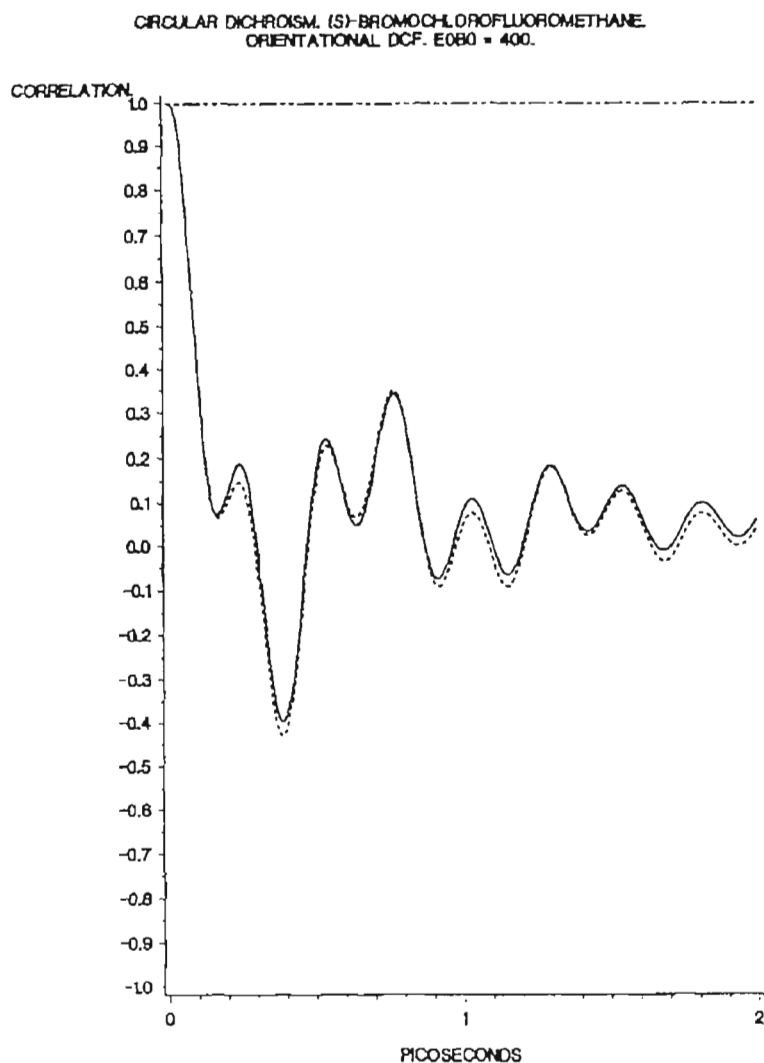


Figure 2

As for Figure (1), orientational DCF's.

Rosenfeld tensor in the bromochlorofluoromethanes:

$$\begin{aligned} \alpha''_{2,11} : \alpha''_{2,22} : \alpha''_{2,33}(S) \\ = 1 : 2 : 3 \quad (S) \\ = -(1 : 2 : 3) \quad (R) \end{aligned} \quad (27)$$

i.e. a simple ratio 1:2:3 with each element changing sign between enantiomers. This procedure was considered adequate to demonstrate the existence of DCF's.

The simulation was repeated for several laser frequencies in the visible (one hundred terahertz (THz) range), mimicking the measurement of

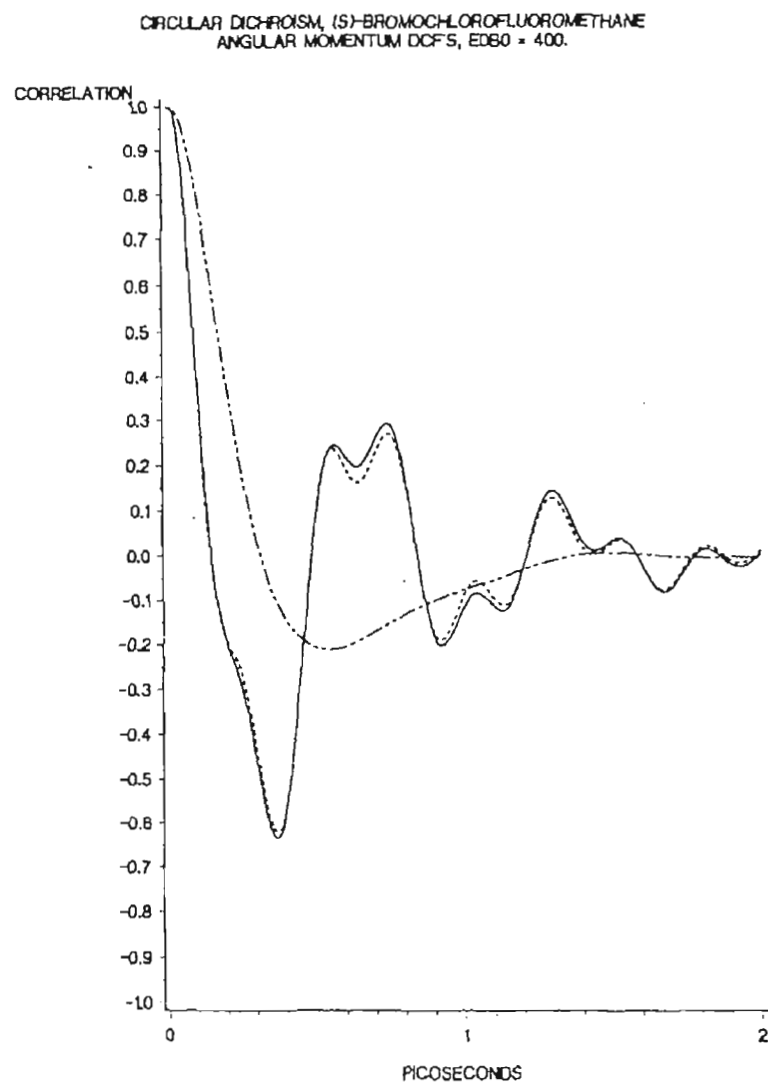


Figure 3

As for Figure (1), angular momentum DCF's.

dichroism and optical rotation at one (laser) frequency. In this way the (classical) simulation was made to mimic a CD and ORD band, rather than monochromatic dichroism and rotation at one laser frequency.

4. RESULTS - THE DIFFERENCE CORRELATION FUNCTIONS AND TRANSIENTS.

Figs (1) to (5) illustrate the DCF's of several molecular vectors. Specifically, Fig (1) illustrates the rotational velocity DCF which is the Fourier Transform of the absorption difference of circular dichroism. In each case the Z component becomes different in time dependence from the

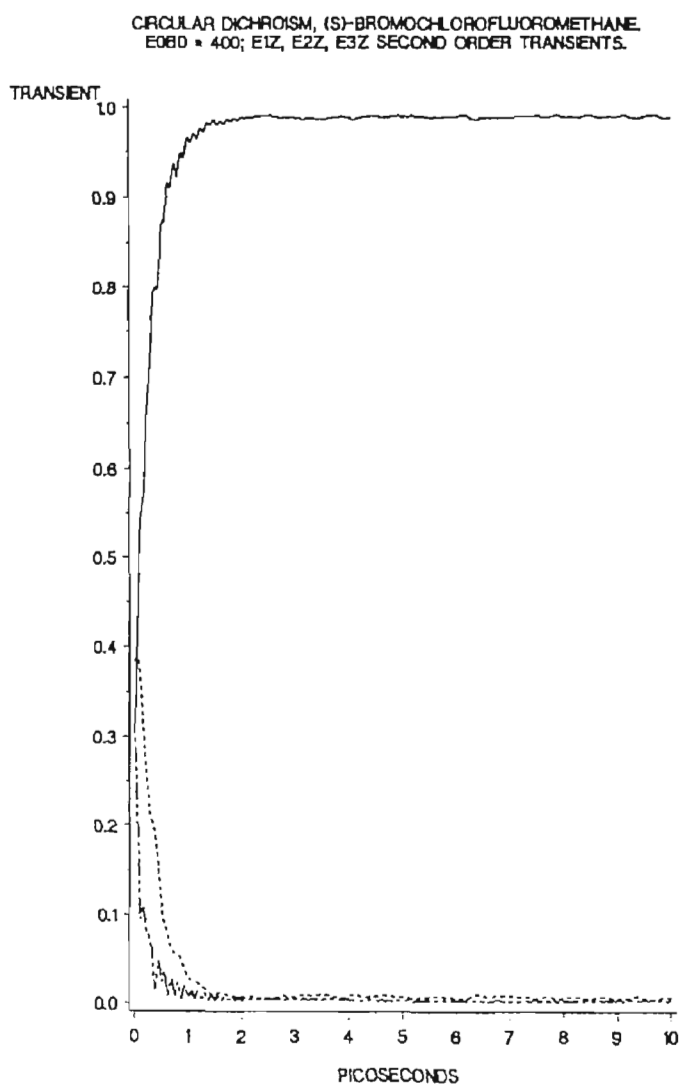


Figure 4

Second order rise transients due to the torque difference (19) of the text. _____ Z component of 1 unit vector of frame (1,2,3): ----- Z component of 2 unit vector; Z component of 3 unit vector.

X and Y components, illustrating the anisotropy that accompanies the development of CD and ORD, both with laser frequencies and broad band frequencies. This is particularly marked in the orientational DCF's of Figure (2), whose component along the Z propagation axis is a slow, monotonic, decay, and the other two components are rapidly oscillating functions with approximately the same time dependence. A similar pattern is observed in the angular momentum DCF's of Fig (3), and in the second and fourth order orientational rise transients of Figs (4) and (5), defined respectively as $\langle e_{1L}^2 \rangle$, $\langle e_{2L}^2 \rangle$ and $\langle e_{3L}^2 \rangle$; and $\langle e_{1L}^4 \rangle$, $\langle e_{2L}^4 \rangle$ and $\langle e_{3L}^4 \rangle$.

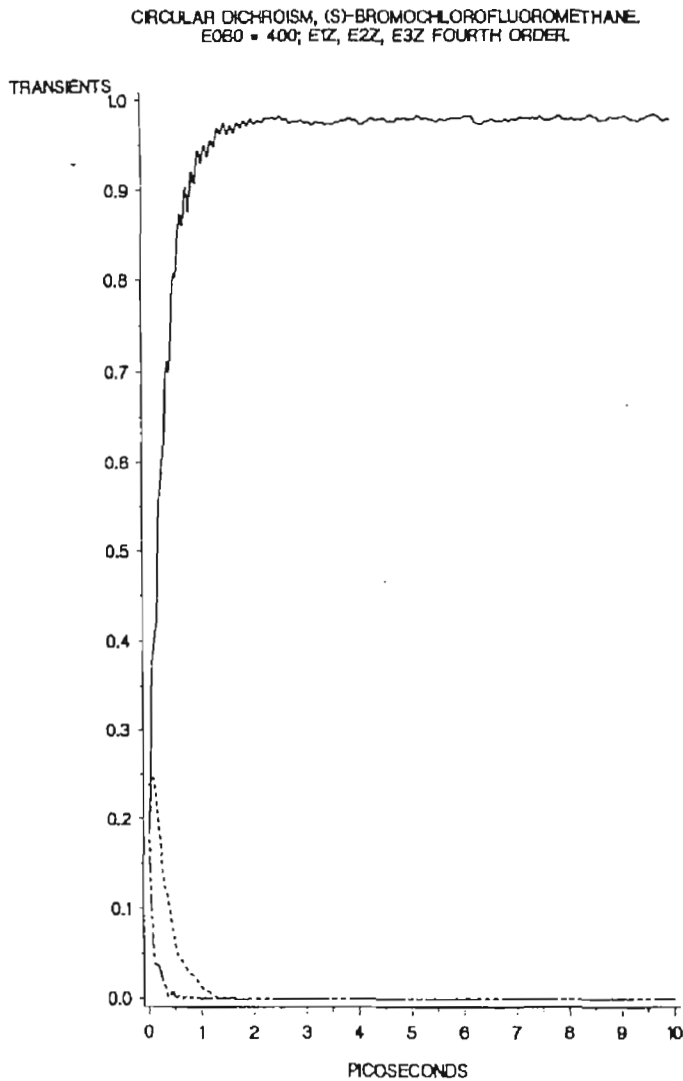


Figure 5

As for Figure 4, fourth order transients.

The DCF's isolated in this paper are given for the purposes of demonstration, and other mechanisms may well contribute to the observed spectrum of circular dichroism and optical rotatory dispersion. These will be presented in future work.

CONCLUSION

Field applied molecular dynamics computer simulation has been used for the first time to isolate the pseudo-scalar correlation function responsible fundamentally for circular dichroism (CD) and optical rotary dispersion (ORD).

ACKNOWLEDGEMENTS

The Swiss NSF is acknowledged for funding this project, and ETH Zurich for a grant of computer time on the IBM 3090 supercomputer. Prof. Dr. G. Wagnière and Prof. Dr. S. Wozniak are thanked for discussions, and Dr. L. J. Evans for help with the SAS plotting facilities of the University of Zurich mainframe.

REFERENCES

- (1) L. D. Barron. "Molecular Light Scattering and Optical Activity, (Cambridge Univ. Press, Cambridge, 1982).
- (2) P. W. Atkins, "Molecular Quantum Mechanics", (Oxford Univ. Press, Oxford, 1983, 2nd ed.)
- (3) S. Kielich, in M. Davies (senior reporter) "Dielectric and Related Molecular Processes", (Chemical Society, London, 1972), vol. 1.
- (4) M. W. Evans, *Physica B*, 168 (1991) 9.
- (5) M. W. Evans, *J. Chem Phys.*, 76 (1982) 5473, 5480.
- (6) M. W. Evans, *J Chem Phys.*, 77 (1982) 4632; 78 (1983) 925, 79 (1983) 5403.
- (7) M. W. Evans, G. C. Lie, and E. Clementi, *J. Chem. Phys.*, 87 (1987) 6040.
- (8) M. W. Evans and G. Wagniere, *Phys. Rev. A*, 42 (1990) 6732.

- (9) M. W. Evans, W. T. Coffey, and P. Grigolini, "Molecular Diffusion" (Wiley Interscience, New York, 1984, M.I.R., Moscow, 1988) Chapters 1 & 2.
- (10) M. W. Evans, P. Grigolini, G. Pastori, I. Prigogine and S. A. Rice (eds.), "Advances in Chemical Physics" (Wiley Interscience, New York, 1985). Vol 62, Chapters 5 and 6.
- (11) M. W. Evans, G. J. Evans, W. T. Coffey and P. Grigolini, "Molecular Dynamics" (Wiley Interscience, New York, 1982), Chapter 1.
- (12) M. W. Evans, Phys. Rev. Lett., 50 (1983) 351.
- (13) S. Kielich, "Non-Linear Molecular Optics", (Nauka, Moscow, 1981).
- (14) M. W. Evans, S. Woźniak and G. Wagnière, Physica B, in press.
- (15) M. W. Evans and D. M. Heyes, Mol. Phys., 69 (1990) 241.
- (16) S. Woźniak, B. Linder, and R. Zawodny, J. Phys., Paris, 44 (1983) 403.
- (17) E. P. Wigner, "Group Theory", (Academic, New York, 1959).
- (18) M. W. Evans, J. Chem. Soc., Faraday 2, 79 (1983) 1811.
- (19) M. W. Evans, Phys. Scripta, 30 (1984) 94.
- (20) M. W. Evans, J. Chem. Soc, Faraday 2, 81 (1985) 1463.
- (21) M. W. Evans, Phys. Rev. Lett., 55 (1985) 1551.
- (22) M. W. Evans, J. Chem. Soc., Faraday 2, 70 (1974) 477.
- (23) M. W. Evans, Phys. Lett. A, 102 (1984) 248.
- (24) M. W. Evans, Phys. Rev. A, 30 (1984) 2062.
- (25) M. W. Evans, G. C. Lie and E. Clementi, IBM Technical Report, KGN 153 (1988).
- (26) M. W. Evans and D. M. Heyes, Mol. Phys., 65 (1988) 1441.
- (27) M. W. Evans, in I. Prigogine and S. A. Rice (eds.), "Advances in Chemical Physics" (Wiley Interscience, New York, 1991), vol. 81.